JOURNAL OF AIRCRAFT
Vol. 47, No. 3, May–June 2010

Reliability-Based Design Optimization of Nonlinear Aeroelasticity Problems

Samy Missoum* and Christoph Dribusch†
University of Arizona, Tucson, Arizona 85721
and
Philip Beran‡
U.S. Air Force Research Laboratory, Wright-Patterson Air Force Base, Ohio 45433

DOI: 10.2514/1.46665

This paper introduces a methodology for the reliability-based design optimization of systems with nonlinear aeroelastic constraints. The approach is based on the construction of explicit flutter and subcritical limit cycle oscillation boundaries in terms of deterministic and random design variables. The boundaries are constructed using a support vector machine that provides a way to efficiently evaluate probabilities of failure and solve the reliability-based design optimization problem. Another major advantage of the approach is that it efficiently manages the discontinuities that might appear during subcritical limit cycle oscillations. The proposed approach is applied to the construction of flutter and subcritical limit cycle oscillation boundaries for a two-degree-of-freedom airfoil with nonlinear stiffnesses. The solution of a reliability-based design optimization problem with a constraint on the probability of subcritical limit cycle oscillation is also provided.

I. Introduction

THE optimal design of systems with aeroelastic constraints faces several hurdles that often originate from the presence of nonlinearities. Among the nonlinear phenomena, limit cycle oscillations (LCOs) [1,2] have emerged as an interesting design challenge.

The LCO phenomenon is characterized by periodic oscillations of generally moderate amplitude. It is usually not a dramatic event, but LCOs might hamper, for instance, control and maneuverability. In some cases, LCOs can also be a fortunate alternative to otherwise unstable behaviors. However, from a design point of view, the challenge lies in developing approaches to manage LCOs and mitigate their effects in a way prescribed by the designer.

It is commonly accepted that two situations might be associated with LCO:

1) In the transonic regime, shock waves can trigger LCOs. Wing configurations involving stores and missiles (e.g., F-16) are particularly prone to LCOs [3].

2) Structural nonlinearities can lead to LCOs by inducing instabilities. Such nonlinearities are found in high-aspect-ratio wings, such as those found in high-altitude surveillance airplanes, and are characterized by a high flexibility and large deformations [4].

Therefore, LCOs are sustained by either aerodynamic nonlinearities and/or structural nonlinearities [5]. In some situations, it might be difficult to clearly separate the contribution of these two factors. Studies have typically focused on one or the other [1,2,4]. In this paper, we will only consider LCOs due to structural nonlinearities.

One of the difficulties of designing for LCOs is their subcritical or supercritical nature. This qualifies the fact that oscillations appear either before or after the flutter velocity (Fig. 1). Subcritical LCOs require a special treatment in aeroelastic design, not only because they appear before the critical flutter velocity, but also because they lead to discontinuous responses that hamper the use of classical computational design tools for optimization or reliability assessment.

Because of the presence of nonlinearities, the aeroelastic behavior (flutter and LCO) might be highly sensitive to uncertainties, which must be accounted for in a proper aeroelastic design process. Several publications can be found in the area of uncertainty quantification for either general aeroelasticity problems [6] or LCOs specifically [7–9]. Other studies on aeroelastic design optimization can also be found [10,11]. However, the specificity of LCO problems and the corresponding discontinuous behavior have not been addressed in a probabilistic design optimization context.

In this paper, we propose a probabilistic optimization method that can efficiently handle flutter and LCO constraints. This is done by constructing multidimensional explicit boundaries for flutter and subcritical LCOs in terms of variables. The variables can be directly related to the design (e.g., a stiffness) or loads and flight conditions (e.g., angle of attack). The proposed approach differs widely from traditional design of experiment (DOE) and metamodeling approaches [12–14], because responses (e.g., LCO amplitude) are not approximated but only classified as acceptable or not. The latter feature is essential for problems with discontinuous behaviors or binary behaviors (accept or reject). This was demonstrated by the first author for crashworthiness and buckling problems [15,16] as well as biomedical device design [17]. The explicit boundaries are created using a support vector machine (SVM) that can create multidimensional, nonlinear, and disjoint boundaries. SVM belongs to the class of classifiers and is widely used in the computer science community [18,19]. The SVM boundary is constructed from an initial DOE whose samples are classified into two categories based on the response of the system.

In the case of aeroelasticity problems, the responses are quantified and qualified differently for flutter and subcritical LCO constraints. For flutter, a stable or unstable status is assigned to a specific configuration. The classification of the configurations as stable or unstable can be performed in two ways: through spectral analysis of the Jacobian (when available) or a stability analysis based on the time history of the mechanical energy. Section III provides details about these two approaches. For LCOs, discontinuities are detected using a clustering technique (e.g., K-means [20]), which leads to the formation of two classes. This is used to directly generate the subcritical LCO boundary (Sec. IV).

Received 8 August 2009; revision received 7 January 2010; accepted for publication 1 February 2010.

*Assistant Professor, Aerospace and Mechanical Engineering, P.O. Box 210119. Member AIAA.
†Research Assistant, Aerospace and Mechanical Engineering, P.O. Box 210119. Student Member AIAA.
‡Principal Research Aerospace Engineer, Design and Analysis Methods Branch. Member AIAA.

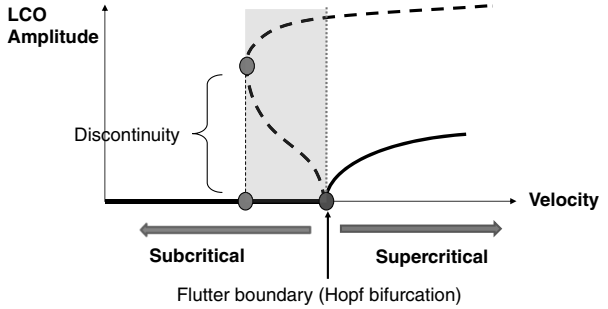

Fig. 1 LCO amplitude in the sub- and supercritical regions.

Once the explicit boundaries are constructed, they are used to calculate probabilities of failure through efficiently evaluated Monte Carlo simulation (MCS). These estimates can then be used to perform reliability-based design optimization (RBDO) [15] as described in Sec. V.

The proposed methodology is demonstrated on a simple airfoil with two degrees of freedom (DOF) in pitch and plunge [21]. The first set of results deals with the construction of explicit flutter boundaries for an airfoil with linear behavior. The stability analysis is carried based on the Jacobian and on the time history of the mechanical energy. The second set of results concerns the construction of explicit subcritical LCO boundary for the airfoil problem with nonlinear stiffnesses. The LCO boundary is subsequently included in an RBDO problem with a constraint on the probability of occurrence of subcritical LCOs.

II. Explicit Design Space Decomposition

The central approach of the proposed methodology is referred to as explicit design space decomposition (EDSD) [15], whereby the boundaries of failure (or infeasible) regions are defined explicitly with respect to the variables. The approach consists of classifying the designs as acceptable and unacceptable and explicitly defining the boundaries that separate them. Therefore, the approach does not approximate responses, as traditionally done, but classifies them. Figure 2 provides an example of design space decomposition.

The explicit boundaries are obtained using an SVM classifier [18,19]. This technique is general, as it allows the definition of explicit nonlinear boundaries in a multidimensional space and can form disjoint regions. More specifically, consider a set of N training points $\mathbf{x}_i$. Each point is associated with one of two classes characterized by a value $y_i = \pm 1$. A general expression of the SVM is

$$s = b + \sum_{i=1}^{N} \lambda_i y_i K(\mathbf{x}_i, \mathbf{x}) \tag{1}$$

where λ_i are Lagrange multipliers, b is a scalar determined by quadratic programming optimization, and s is negative or positive,

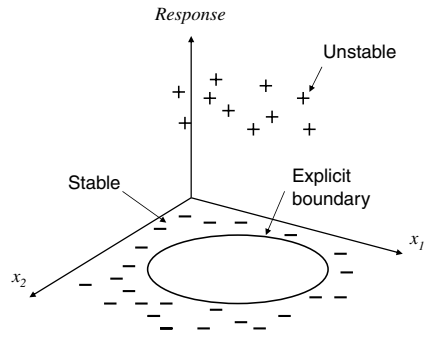

Fig. 2 Example of explicit boundaries in the design space (x_1, x_2) delimiting stable and unstable system behaviors.

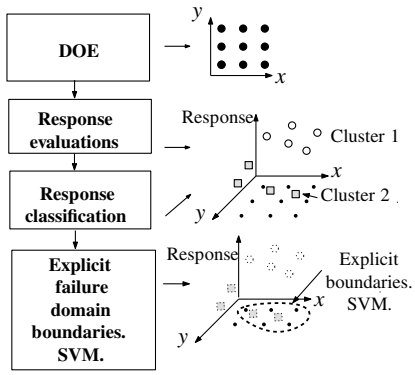

Fig. 3 Basic methodology of explicit design space decomposition using SVM.

depending on the predicted class. Several types of kernel exist, such as polynomial, radial basis, etc. [18]. In this study we use the Gaussian kernel, but this choice is not essential, as other kernels would lead to very similar results:

$$K(\mathbf{x}_i, \mathbf{x}) = \exp\left(-\frac{\|\mathbf{x}_i - \mathbf{x}\|^2}{2\sigma^2}\right) \tag{2}$$

where σ is a width parameter of the kernel.

Figure 3 provides an overview of the EDSD methodology:

1) Perform a uniform DOE, such as centroidal voronoi tesselation (CVT) [22], with the chosen design variables. In a perfectly uniform DOE, the Euclidean distance between each pair of samples is identical.

2) Evaluate the state of the system with a simulation for each DOE sample. Classify them as acceptable or unacceptable.

3) Define the explicit boundaries of the failure regions using SVM.

To minimize the number of function evaluations required for the training of the SVM and obtain an accurate boundary, an adaptive sampling scheme was introduced by the authors [23]. This refinement is essential for the scalability of the EDSD approach in high-dimensional spaces.

III. Classification for the Construction of an SVM Explicit Flutter Boundary

This section describes the construction of explicit flutter (stability) boundaries in terms of deterministic and/or random variables using EDSD. The classification used to train the SVM consists of classifying the samples into stable and unstable configurations. This classification is performed in two ways. The first approach assumes the availability of the Jacobian (or its approximation) for a spectral analysis. The second approach is based on the transient response of the system and is best suited for problems involving black-box simulations.

A. Stability Analysis Based on the Jacobian

Consider a system governed by a set of n first-order differential equations:

$$\mathbf{X}' = \mathbf{f}(\mathbf{X}; \mathbf{p}) \tag{3}$$

where $\mathbf{p}$ is a vector of parameters. At equilibrium, we have $\mathbf{f}(\mathbf{X}; \mathbf{p}) = \mathbf{0}$. Based on linear stability theory, the n eigenvalues λ_i of the Jacobian $\mathbf{J}$ of component $J_{ij} = \partial f_i / \partial X_j$ provide the following information on the stability of the system at equilibrium:

1) If $\Re(\lambda_i) < 0 \ \forall \ i$, the system is stable.

2) If $\exists \ i \ \Re(\lambda_i) > 0$, the system is unstable.

It is therefore possible to classify a system configuration as stable or unstable by evaluating the sign of the maximum real part of the eigenvalues. Each sample $\mathbf{X}_i$ of the DOE is then assigned a value $y_i = \text{sgn}(\max(\Re(\lambda_i)))$ (i.e., $y_i = \pm 1$) for the training of the SVM.

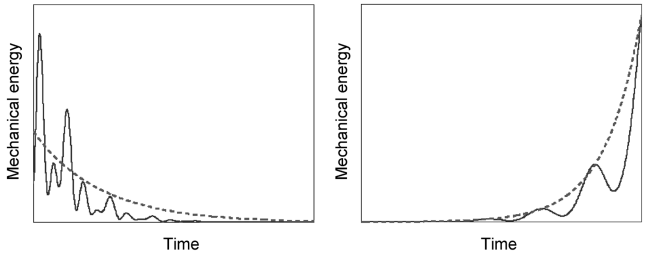

Fig. 4 Mechanical energy for a stable (left) and an unstable configuration (right). The dashed line represents an exponential least-squares approximation whose exponent p_2 is either positive (unstable) or negative (stable).

Note that in problems involving LCOs, the flutter point is a Hopf bifurcation [21,24]. It represents the transition from a stable equilibrium to an oscillatory behavior. A Hopf bifurcation is characterized by one, and only one, pair of conjugate eigenvalues $(\lambda, \bar{\lambda})$ of the Jacobian with vanishing real part, and at an equilibrium point $(\mathbf{X_E}, \mathbf{p}^*)$, the transversality condition must be satisfied: $\mathrm{d}\Re(\lambda)/\mathrm{d}p_i \neq 0$.

B. Stability Analysis Based on the Mechanical Energy

Another approach to assess the stability of a given configuration consists of studying its response in the time domain. This approach is essential in the case of black-box codes for which the Jacobian is not available. In addition, the study of the system's response is the only way to assess the true stability boundary (as opposed to based on a linear assumption) of a nonlinear system in the general case.

In this study, the response considered is the mechanical energy defined as the sum of the kinetic and the elastic energies. This approach has the advantage of encompassing all the degrees of freedom of the systems in one quantity. For an asymptotically stable system, the energy will converge. For an unstable system, the system energy will continue to grow unboundedly. To capture the trend, the following function,

$$y(\tau) = p_1 e^{p_2 \tau} \tag{4}$$

with parameters p_1 and p_2, approximates (in a least-squares sense) the peaks of the mechanical energy. If p_2 is negative, the system is classified as stable; otherwise, it is unstable. From this, each sample of the DOE is assigned a class $y_i = \pm 1$. Figure 4 provides examples of stable and unstable configurations. An example of calculation of the mechanical energy is provided in Sec. VI.B.2 for a two-degree-of-freedom system.

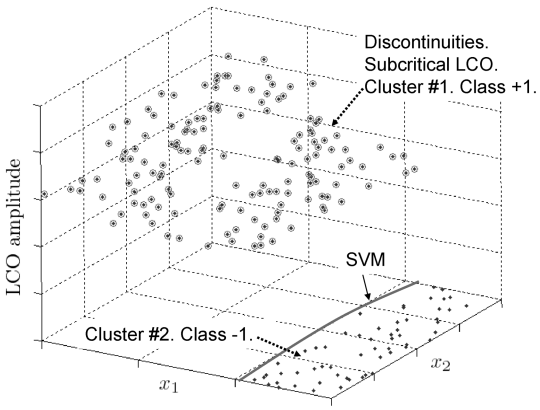

Fig. 5 Schematic representation of classification of discontinuous subcritical LCO amplitude using two clusters for two generic variables x_1 and x_2. The clusters are identified automatically using *K*-means, therefore allowing the construction of an SVM explicit boundary.

IV. Classification for the Construction of an Explicit Subcritical LCO Boundary

The subcritical LCOs appearing before the flutter point are characterized by a discontinuity in amplitude, as presented in Fig. 1. This discontinuity can therefore be used as a way of classifying the DOE samples into subcritical LCOs or not. The discontinuous behavior can be efficiently identified by a clustering technique such as *K*-means [20]. The *K*-means algorithm identifies an a priori given number of clusters. This is done by minimizing the sum of the distances of the samples in a cluster to its centroid. In the problem of isolating the subcritical discontinuities, two clusters only must be identified. It is noteworthy that cluster identification can be difficult in a multidimensional space. However, in this work, the DOE is close to uniform and only one response is used, thus simplifying the clustering. In fact, for a perfectly uniform DOE, the cluster identification could be reduced to a one-dimensional problem using the amplitude response only. This classification of the amplitude in two clusters provides a natural way of constructing an explicit boundary for subcritical LCOs. Based on its cluster, a DOE sample will be assigned a $y_i = \pm 1$ value for the training of SVM. Figure 5 provides a schematic explanation of the methodology.

V. RBDO Solution Scheme

We consider the following formulation of RBDO problem:

$$\min_{\bar{x}} \quad f(\bar{x}) \tag{5a}$$

$$\text{subject to} \quad P(x \in \Omega_f) \leq P_T \tag{5b}$$

where P_T is the target probability, x is a vector of random variables, and the bar sign represents the mean. That is, the optimization search is carried out with respect to the mean of the variables, and the probability of failure is assessed based on the probabilistic distribution of the variables. Ω_f is the failure domain in which boundaries are defined with an SVM. Examples of failure domains are the regions where subcritical LCOs occurs or instability regions.

The calculation of the probability of failure P_f can be achieved through approximation schemes such as MCS, first- and second-order reliability method, and advanced-mean value [25,26]. In the proposed SVM-based approach it is natural to use MCS, because the evaluation of the state of a Monte Carlo sample through Eq. (1) is very efficient. However, the inclusion of a brute-force MCS process within an optimization loop is not recommended for three main reasons:

1) It is relatively time-consuming.

2) The probability calculated by MCS is noisy due to the randomness of the sampling.

3) The probabilities are typically low and can vary by orders of magnitude during the optimization process.

To regularize the probabilistic constraint, the reliability index β is used:

$$\beta = -\Phi^{-1}(P_f) \tag{6}$$

where Φ is the standard normal cumulative distribution function.

The reliability index is then approximated by support vector regression [27]. The approximation is constructed by calculating the probability of failure and the corresponding reliability index at each DOE sample initially used to construct the SVM boundary. This approximation is then used to solve the optimization problem whose objective function and constraints are explicit function of the variables. This approximated optimization problem is formally written as

$$\min_{\bar{x}} \quad f(\bar{x}) \tag{7a}$$

$$\text{subject to} \quad \tilde{\beta}(x) \geq \beta_T \tag{7b}$$

where $\tilde{\beta}$ is the approximation of the reliability index and β_T is the index value for the target probability P_T. The optimization can then

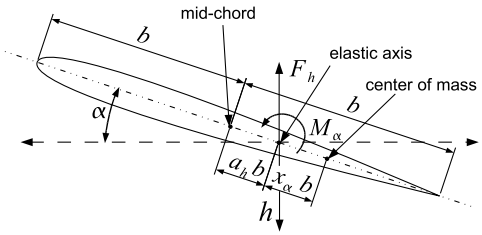

Fig. 6 Description of the two-degree-of-freedom airfoil [21].

be solved using a gradient-based method such as sequential quadratic programming (SQP) or global methods if local optima are present [15,16] without requiring any further aeroelasticity analysis.

VI. Test Examples

The proposed methodology will be demonstrated on a 2-DOF airfoil in the following cases:

1) Construction of a flutter boundary for a linear configuration for which the Jacobian is available analytically as described in Sec. III.A.

2) Construction of a flutter boundary for a linear configuration based on the time history of the mechanical energy as described in Sec. III.B.

3) Construction of a subcritical LCO boundary for a configuration with structural (stiffness) nonlinearities as described in Sec. IV.

4) Solution of an RBDO problem, as described in Sec. V, with a constraint on the probability of occurrence of subcritical LCOs.

A. Airfoil Problem

The problem consists of a 2-DOF airfoil (Fig. 6). The DOF are the pitch angle α and the plunge displacement h. The stiffnesses in pitch and plunge are assumed to be polynomials leading to the following form for the restoring moment M_α and force F_h:

$$M_\alpha = K_\alpha(\alpha + k_{3\alpha}\alpha^3 + k_{5\alpha}\alpha^5) \qquad F_h = K_h(\xi + k_{3h}\xi^3 + k_{5h}\xi^5) \quad (8)$$

where $\xi = h/b$ is the nondimensional plunge. As mentioned in the Introduction, these nonlinear stiffness properties (representative of structural geometric nonlinearities for actual wings) make LCOs possible. The stiffness terms $k_{3\alpha}$,$k_{5\alpha}$, k_{3h}, and k_{5h} provide the relative importance of the nonlinear terms in comparison with the linear terms. A softening spring (e.g., $k_{3\alpha} < 0$) can lead to subcritical LCOs, whereas a hardening spring (e.g., $k_{3\alpha} > 0$) will lead to supercritical LCOs. Details of the behavior are provided in Sec. VI.C.

The aeroelastic equations of motion were derived in the linear elastic case by Fung [28]. In the nonlinear case, Lee et al. [21] derived the equations for cubic stiffnesses. In this paper, we use identical equations of motion with the addition of a pentic stiffness term in pitch. The pentic stiffness in plunge is set to zero. Incompressible flow is assumed.

A system of eight first-order differential equations is obtained for which the Jacobian is available analytically [21]. The time integration was performed using the explicit Euler method. The code was fully parameterized with respect to the following quantities:

Table 1 Airfoil reference configuration for the construction of flutter boundaries

Initial pitch	0.05
Initial plunge	0.0
Reduced velocity	6.0
Mass ratio	40
Elastic-axis midchord separation a_h	−2.0
Center-of-mass elastic-axis separation x_α	1.8
Radius of gyration r_α	1.8655
Initial velocities	0
Damping in pitch and plunge	0
Nonlinear stiffnesses	0

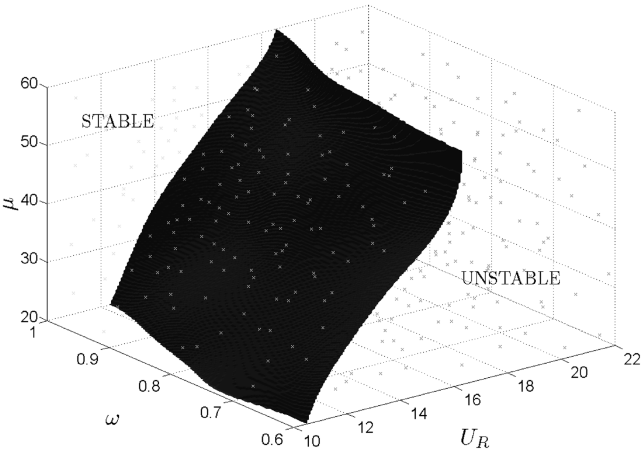

Fig. 7 SVM flutter boundary as a function of the natural frequency ratio ω, the reduced velocity U_R, and the mass ratio μ.

initial pitch α_0, initial plunge ξ_0, reduced velocity U_R, airfoil-to-air mass ratio $\mu = m/\pi\rho b^2$, natural frequency ratio $\omega = \omega_{\text{plunge}}/\omega_{\text{pitch}}$, radius of gyration r_α, airfoil geometry parameters as depicted in Fig. 6, and stiffnesses.

B. Construction of Flutter Boundaries for the Airfoil Problem

To generate the linear flutter boundary, a CVT DOE was generated with 1000 samples based on the variations of three variables: ω, μ, and U_R. For the sake of comparison, the boundary was generated using the eigenvalues and using the time history of the system energy. A list of numerical values of other fixed parameters is provided in Table 1.

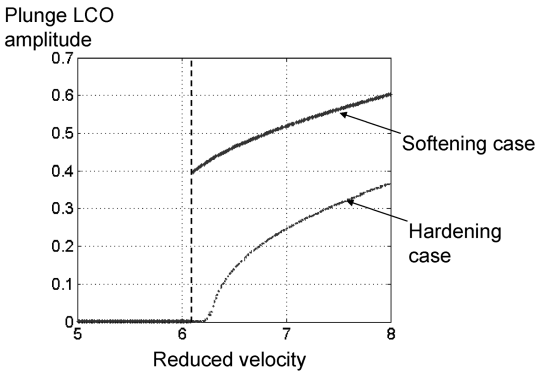

Fig. 8 Plunge amplitude for a softening ($k_{3\alpha} = -3 < 0$) and for a hardening case ($k_{3\alpha} = +3 > 0$). The dashed line shows for which reduced velocity the discontinuity occurs (before the flutter point).

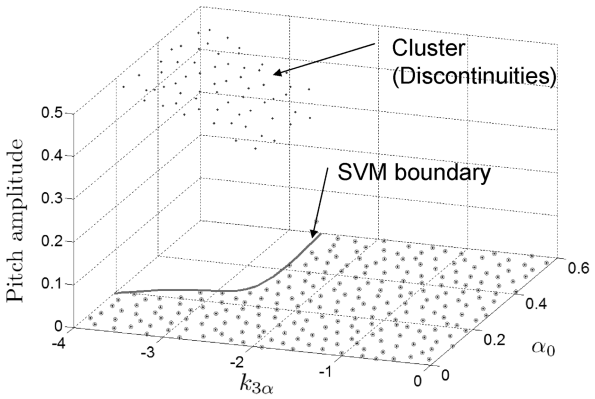

Fig. 9 Pitch amplitude as a function of the initial angle of attack and the pitch cubic stiffness. The subcritical LCO boundary confirms the intuitive expectation that subcritical LCOs only occur for a softening spring and perturbed initial conditions.

Table 2 Airfoil reference configuration for LCO boundaries

Initial plunge	0.0
Reduced velocity	6.0
Mass ratio	100
Natural frequency ratio	0.2
Elastic-axis midchord separation a_h	−0.5
Center-of-mass elastic-axis separation x_α	0.25
Radius of gyration r_α	0.5
Initial velocities	0
Damping in pitch and plunge	0
Pentic stiffness	20

1. Classification Based on Spectral Analysis

For the airfoil problem, the Jacobian is readily available analytically [21], so the extraction of eigenvalues λ_i is straightforward. The samples are classified as described in Sec. III.A for the construction of the SVM-based explicit flutter boundary.

2. Classification Based on Mechanical Energy

For the same linear configuration, the stability analysis was performed using the approach based on time history of the energy of the system (Sec. III.B). The system energy is calculated from the pitch and plunge velocities and the deformation of the springs. For the 2-DOF system, the classification is not based on the system energy E directly, but on the dimensionless system energy $\bar{E}$, defined by

$$\bar{E} = \frac{E}{\rho U^2 b^2} \tag{9}$$

The energy stored in the spring in plunge is calculated as

$$\bar{E}_{\text{spring}\xi} = \mu\pi\left(\frac{\omega}{U_R}\right)^2\left(\frac{1}{2}\xi^2 + \frac{1}{4}k_{3h}\xi^4 + \frac{1}{6}k_{5h}\xi^6\right) \tag{10}$$

Similarly, for the spring in pitch,

$$\bar{E}_{\text{spring}\alpha} = \mu\pi\left(\frac{r_\alpha}{U_R}\right)^2\left(\frac{1}{2}\alpha^2 + \frac{1}{4}k_{3\alpha}\alpha^4 + \frac{1}{6}k_{5\alpha}\alpha^6\right) \tag{11}$$

The kinetic energies are calculated as

$$\bar{E}_{\text{kinetic}\xi} = \tfrac{1}{2}\mu\pi\xi'^2 + 2x_\alpha\alpha'\xi'\cos(\alpha) + (x_\alpha\alpha')^2 \tag{12}$$

$$\bar{E}_{\text{kinetic}\alpha} = \tfrac{1}{2}\mu\pi U_R^2\alpha'^2 \tag{13}$$

where the prime notation represents the derivative with respect to the nondimensional time $\tau = Ut/b$. Note that we are considering a linear behavior, so the terms of degree larger than 2 in Eqs. (10) and (11) are set to zero. The two approaches used for the construction of the explicit linear flutter boundary lead to identical classifications and SVM surfaces (Fig. 7).

C. Subcritical LCO Boundary: Airfoil Problem

Subcritical LCOs are characterized by a discontinuity in amplitude. In the case of the airfoil problem, this means a discontinuity from the equilibrium state (i.e., $\mathbf{X} = \mathbf{0}$) to oscillations occurring before the linear flutter boundary. Figure 8 provides a depiction of the discontinuity of the response as a function of the reduced velocity for the softening and hardening case.

These discontinuities, detected by the K-means clustering algorithm, enable the classification of the responses for SVM. Figure 9 depicts the pitch amplitude with respect to the initial angle of attack α_0 and the pitch cubic stiffness $k_{3\alpha}$. This was done for a reference configuration given in Table 2. The boundary depicted in Fig. 9 can be physically interpreted as follows: no LCOs can appear for a zero initial angle of attack. In other words, the system is in equilibrium (zero amplitude). LCOs occur starting from a certain negative value of the stiffness (i.e., a softening spring) and value of the initial angle of attack. For an increasingly softening spring, LCOs will occur for smaller values of the initial angle of attack.

The construction of the subcritical SVM boundary was extended to a problem with three variables by adding the plunge cubic stiffness. The corresponding boundary is depicted in Fig. 10. The other parameters of the problem are given in Table 2. Figure 10 confirms that the occurrence of subcritical LCOs requires both a softening spring and an initial perturbation from the equilibrium configuration.

VII. Reliability-Based Design Optimization with the Airfoil Problem

Once the subcritical LCO boundary is obtained explicitly, it is possible to efficiently solve an RBDO problem as described in Sec. V. The RBDO methodology is applied to a nonlinear aeroelasticity optimization based on the 2-DOF airfoil. The problem considered is the minimization of the sum of cubic stiffnesses while avoiding subcritical LCOs with a given target probability P_T. The design variables are the cubic plunge and pitch stiffnesses, which are considered as normally distributed. In addition, the initial pitch is a random variable with uniform distribution as the values of the angle of attack are assumed equiprobable. The optimization problem is

$$\min_{\bar{k}_{3\alpha},\bar{k}_{3h}} \quad \bar{k}_{3\alpha} + \bar{k}_{3h} \tag{14a}$$

$$\text{subject to} \quad P((k_{3\alpha}, k_{3h}, \alpha_0) \in \Omega_f) \le P_T \tag{14b}$$

where the bar sign represents the mean. Ω_f is the three-dimensional failure domain where subcritical LCOs occur as depicted in the previous section (Fig. 10).

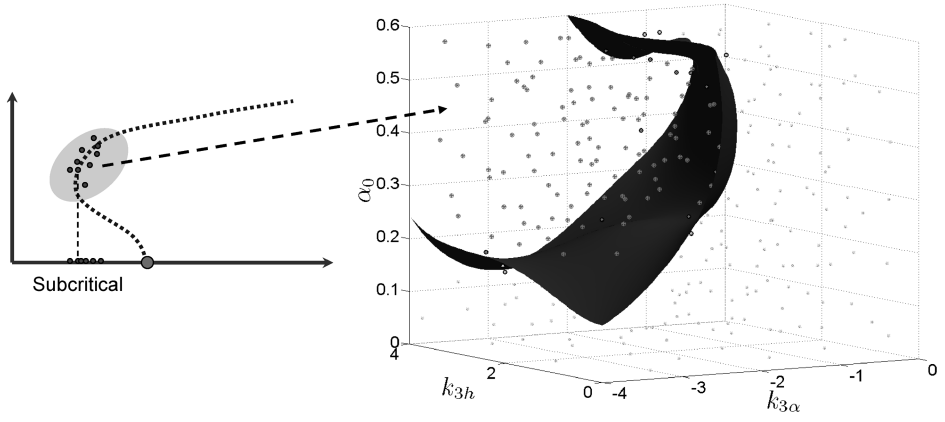

Fig. 10 Subcritical LCO boundary as a function of the angle of attack, and the pitch and cubic stiffnesses. Again, subcritical LCOs only occur for a softening spring and perturbed initial conditions.

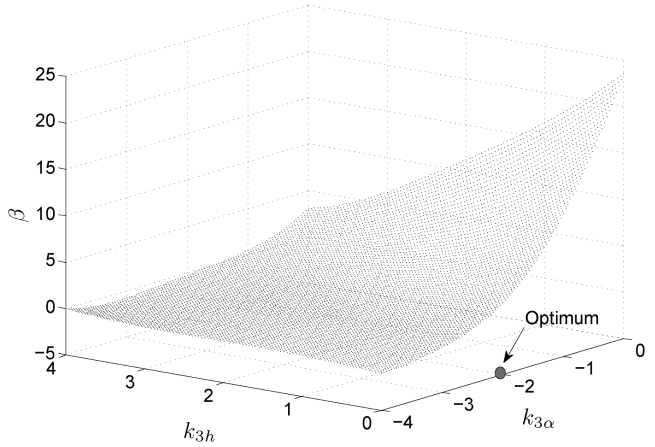

Fig. 11 Approximation of the reliability index and optimal solution.

Note that the choice of the objective function was motivated by the fact that a traditional objective is to minimize weight. However, in the airfoil problem, the only design modifications possible are the stiffnesses. The proposed objective function assumes that stiffness reduces when the weight reduces. This assumption does not remove any generality to the methodology. In fact, models for which some design variables are explicitly related to the weight (e.g., a finite element model) could also be used.

The target probability P_T is set to 10^{-3} and probabilities of failure are calculated based on 10^5 samples. The distributions and ranges of the random variables are $k_{3\alpha} \in [-4, 0]$: $N(\bar{k}_{3\alpha}, 0.15)$, $k_{3h} \in [0, 4]$: $N(\bar{k}_{3h}, 0.15)$, and α_0: $U(0, 0.6)$.

As described in Sec. V, in order to perform the optimization, the probabilities, calculated at the DOE samples, are transformed into the corresponding reliability indices. The reliability index over the whole search space is then obtained through approximation (Fig. 11). The optimization is then performed using SQP to reach the following optimum $k_{3\alpha} = -1.927$ and $k_{3h} = 0.0$ for which the probabilistic constraint is active. The actual probability of failure at the predicted optimum, based on MCS, is 5.7×10^{-4}. Figure 11 depicts the approximated reliability index as well as the optimum solution.

VIII. Conclusions

This paper introduces an approach for the probabilistic optimal design of nonlinear aeroelastic problems. The method relies on the construction of explicit stability (flutter) and LCO boundaries using SVM. The classification used for the construction of SVM makes use of stability properties (e.g., eigenvalue sign) for flutter or the presence of discontinuities for subcritical LCOs. These constructions enable an efficient assessment of probabilities of flutter or LCOs and are used to solve RBDO problems.

The next step of this research will include a larger number of variables and the use of multifidelity approaches to reduce computational expenses.

Acknowledgments

The support of the National Science Foundation (award CMMI-0800117) is gratefully acknowledged for the research dealing with the explicit design space decomposition methodology. This research was mostly conducted in the context of a summer research program in the Air Vehicle Directorate of the U.S. Air Force Research Laboratory at Wright-Patterson Air Force Base through funding from U.S. Air Force Office of Scientific Research (Fariba Fahroo, Program Manager). Support during this period is gratefully acknowledged. Also, the authors would like to acknowledge the fruitful discussions with Michael McFarland and Mohammad Kurdi.

References

[1] Kousen, K., and Bendiksen, O., "Limit Cycle Phenomena in Computational Transonic Aeroelasticity," *Journal of Aircraft*, Vol. 31, No. 6, 1994, pp. 1257–1263. doi:10.2514/3.46644

[2] Dowell, E., and Tang, D., "Nonlinear Aeroelasticity and Unsteady Aerodynamics," *AIAA Journal*, Vol. 40, No. 9, 2002, pp. 1697–1707. doi:10.2514/2.1853

[3] Beran, P., Strganac, T., Kim, K., and Nichkawde, C., "Studies of Store-Induced Limit-Cycle Oscillations Using a Model with Full System Nonlinearities," *Nonlinear Dynamics*, Vol. 37, No. 4, 2004, pp. 323–339. doi:10.1023/B:NODY.0000045544.96418.bf

[4] Patil, M., Hodges, D., and Cesnik, C., "Limit-Cycle Oscillations in High Aspect Ratio Wings," *Journal of Fluids and Structures*, Vol. 15, No. 1, 2001, pp. 107–132. doi:10.1006/jfls.2000.0329

[5] Lee, B., Price, S., and Wong, Y., "Nonlinear Aeroelastic Analysis of Airfoils: Bifurcation and Chaos," *Progress in Aerospace Sciences*, Vol. 35, No. 3, 1999, pp. 205–334. doi:10.1016/S0376-0421(98)00015-3

[6] Pettit, C., "Uncertainty Quantification in Aeroelasticity—Recent Results and Research Challenges," *Journal of Aircraft*, Vol. 41, No. 5, 2004, pp. 1217–1229. doi:10.2514/1.3961

[7] Pettit, C., and Beran, P., "Effects Of Parametric Uncertainty on Airfoil Limit Cycle Oscillation," *Journal of Aircraft*, Vol. 40, No. 5, 2003, pp. 1004–1006. doi:10.2514/2.6889

[8] Pettit, C. and Beran, P., "Polynomial Chaos Expansion Applied to Airfoil Limit Cycle Oscillations," AIAA Paper 2004-1691, 2004.

[9] Beran, P., Pettit, C., and Millman, D., "Uncertainty Quantification of Limit-Cycle Oscillations," *Journal of Computational Physics*, Vol. 217, No. 1, 2006, pp. 217–247. doi:10.1016/j.jcp.2006.03.038

[10] Allen, M., and Maute, K., "Reliability-Based Design Optimization of Aeroelastic Structures," *Structural and Multidisciplinary Optimization*, Vol. 27, No. 4, 2004, pp. 228–242. doi:10.1007/s00158-004-0384-1

[11] Maute, K., Nikbay, M., and Farhat, C., "Sensitivity Analysis and Design Optimization of Three-Dimensional Nonlinear Aeroelastic Systems by the Adjoint Method," *International Journal for Numerical Methods in Engineering*, Vol. 56, No. 6, 2003, pp. 911–933. doi:10.1002/nme.599

[12] Wang, G. G., and Shan, S., "Review of Metamodeling Techniques in Support of Engineering Design Optimization," *Journal of Mechanical Design*, Vol. 129, No. 4, 2007, pp. 370–380. doi:10.1115/1.2429697

[13] Myers, R., and Montgomery, D., *Response Surface Methodology*, 2nd ed., Wiley, New York, 2002.

[14] Montgomery, D., *Design and Analysis of Experiments*, Wiley, New York, 2005.

[15] Basudhar, A., Missoum, S., and Harrison, S., "Limit State Function Identification Using Support Vector Machines for Discontinuous Responses and Disjoint Failure Domains," *Probabilistic Engineering Mechanics*, Vol. 23, No. 1, Jan. 2008, pp. 1–11. doi:10.1016/j.probengmech.2007.08.004

[16] Missoum, S., Ramu, P., and Haftka, R., "A Convex Hull Approach for the Reliability-Based Design Optimization of Nonlinear Transient Dynamic Problems," *Computer Methods in Applied Mechanics and Engineering*, Vol. 196, Nos. 29–30, 2007, pp. 2895–2906. doi:10.1016/j.cma.2006.12.008

[17] Layman, R., Missoum, S., and Vande Geest, J., "Simulation and Probabilistic Failure Prediction of Grafts for Aortic Aneurysm," *Engineering Computations*, Vol. 27, No. 1, 2010, pp. 84–105. doi:10.1108/02644401011008531

[18] Cristianini, N., and Schölkopf, B., "Support Vector Machines and Kernel Methods: The New Generation of Learning Machines," *Artificial Intelligence Magazine*, Vol. 23, No. 3, 2002, pp. 31–41.

[19] Alpaydin, E., *Introduction to Machine Learning*, MIT Press, Cambridge, MA, 2004.

[20] Hartigan, J., and Wong, M., "A *K*-Means Clustering Algorithm," *Applied Statistics*, Vol. 28, 1979, pp. 100–108.

[21] Lee, B., Jiang, L., and Wong, Y., "Flutter of an Airfoil with Cubic Restoring Force," *Journal of Fluids and Structures*, Vol. 13, No. 1, 1999, pp. 75–101. doi:10.1006/jfls.1998.0190

[22] Romero, V., Burkardt, J., Gunzburger, M., and Peterson, J., "Comparison of Pure and 'Latinized' Centroidal Voronoi Tesselation Against Various Other Statistical Sampling Methods," *Reliability Engineering and System Safety*, Vol. 91, Nos. 10–11, 2006, pp. 1266–1280. doi10.1016/j.ress.2005.11.023

[23] Basudhar, A., and Missoum, S., "Adaptive Explicit Decision Functions for Probabilistic Design and Optimization Using Support Vector Machines," *Computers and Structures*, Vol. 86, Nos. 19–20, 2008, pp. 1904–1917. doi:10.1016/j.compstruc.2008.02.008

[24] Morton, S., and Beran, P., "Hopf-Bifurcation Analysis of Airfoil Utter at Transonic Speeds," *Journal of Aircraft*, Vol. 36, No. 2, 1999, pp. 421–429. doi:10.2514/2.2447

[25] Melchers, R., *Structural Reliability Analysis and Prediction*, Wiley, New York, 1999.

[26] Haldar, A., and Mahadevan, S., *Probability, Reliability, and Statistical Methods in Engineering Design*, Wiley, New York, 2000.

[27] Clarke, S., Griebsch, J., and Simpson, T., "Analysis of Support Vector Regression for Approximation of Complex Engineering Analyses," *Journal of Mechanical Design*, Vol. 127, Nov. 2005, pp. 1077–1087. doi:10.1115/1.1897403

[28] Fung, Y., *An Introduction to the Theory of Aeroelasticity*, Courier Dover, New York, 2002.